Testing and Isolation Efficacy: Insights from a Simple Epidemic Model

May 5, 2021

1 Abstract

The effect of testing processes, including (testing and test reporting) on an epidemic dynamics (infection and recovery) can be studied at the individual level or the community level (e.g., nursing homes, long-term-care facilities, etc.). Gaining insights to determine the sensitivity of the epidemic dynamics with respect to the testing processes will depend on underlying factors including the level of focus (individual or community), assumptions (model), and the interplay between these factors. In particular, the fast testing and test reporting may be beneficial at the community-level, supported by many studies, as it gives a rapid assessment of the situation, identifies hot spots, and may enable rapid contact-tracing. However, the potential advantage of a slow rate of test return on the dynamics of an epidemic is real, often neglected, and needs to be quantified. At the individual level, this advantage can manifest in the following sense: individuals awaiting their test results or who have tested positive may partially or fully self-isolate, thus reducing or eliminating their potential in the transmission process. In this paper, we investigated this individual-level effect of testing processes on the epidemic dynamics by developing a SIR-type model. Although the model development was motivated by the COVID-19 epidemic, the model has general epidemiological and testing structures. The realistic components of the model include *per capita* testing intensity, test sensitivity and specificity, rate of test return, and isolation efficacy in reduction of the probability of transmission. The novel component is the compartment-specific relative testing weights, which reflect the testing strategies– surveillance, diagnosis, or control. Here, we compare two testing strategies, random vs. targeted, and concluded that the targeted testing strategy is more effective in the sense that achieving reduction of $\mathcal{R}_0$ can occure in a lower range of testing intensity and longer test return time relative to the random testing. Furthermore, we show that increasing *per capita* testing intensity and reducing the test return time would be beneficial on the dynamics of an epidemic in general but there are exception cases. In particular, it is possible for the basic reproduction number, $\mathcal{R}_0$, to be increasing with respect to the *per capita* testing intensity and the rate of test return when the isolation efficacy in reduction of the probability of transmission for awaiting individuals is loose.

2 Introduction

The observed dynamics of the COVID-19 epidemic are driven by both epidemiological processes (infection and recovery) and testing processes (testing and test reporting). In addition to shaping epidemic observations (via case reports), testing processes can also affect epidemiological dynamics. In particular, individuals with confirmed infections (positive tests) are likely to self-isolate, and individuals who are awaiting the results of a test may do so also (possibly to a lesser extent). We developed a mechanistic model that incorporates epidemic processes and testing in order to explore the effects of testing and isolation on epidemic dynamics.

If testing influences behavior, then epidemic dynamics will depend on patterns of who gets tested. The impacts of testing will depend on intensity (tests performed per day), and on how strongly testing is focused on people who are infectious. This level of focus depends in turn on the purpose and design of testing programs. When testing is done for the purposes of disease surveillance (Foddai et al., 2020) tests should be assigned randomly across the population, possibly with a stratified design for statistical efficiency (Graubard and Korn, 1996) [**Ali:** *a better ref everyone?*].

Over the course of the COVID-19 pandemic, however, the vast majority of testing has been done with other goals – primarily diagnosis (determining the infection status for clinical purposes), or control (determining the infection status in order to quickly isolate cases that have been found by contact tracing), which we characterize as *targeted* testing strategies. In these cases, testing probabilities vary widely across epidemiological compartments; in our dynamical model, we will characterize these probabilities by assigning a *per capita* testing weight to each compartment that determines the *relative* probability that an individual in that compartment will be selected for testing (see Methods).

When testing is used primarily for diagnosis it will focus on people with infection-like symptoms; thus the relative testing weights for infected people will depend on the relative probability of infected people having symptoms. For COVID-19 infection, the testing weights will depend on the relative asymptomatic infections, time spent pre-sympomatic vs. symptomatic infections – and also the incidence of COVID-19-like symptoms among people in the population *not* infected with COVID-19. Testing for epidemic control will focus on people who are known to have been in contact with known infected cases; in this case the testing weights for infected vs. uninfected people will depend on the probability of infection given contact, as well as the thoroughness and effectiveness of the system for identifying suspicious contacts.

The main interest from the epidemiological point of view is to know whether the number of infected individuals goes through an exponential growth phase, following the introduction of an infection in a totally susciptable population, before the disease becomes extinct. This is determined by studying the basic reproduction number $\mathcal{R}_0$. It is defined as the expected number of secondary infections arising from a typical infective individual in a completely susceptible population (Dietz, 1993). In the early stages of an epidemic the number of infected individuals is expected to grow exponentially over time when $\mathcal{R}_0 > 1$, and to decline over time when $\mathcal{R}_0 < 1$. Although the value of $\mathcal{R}_0$ cannot completely characterize the dynamics of even the simplest epidemic model (Shaw and Kennedy, 2021), it does give a simple and widely accepted index for the difficulty of control, as well as some indication

of the likely final size of an epidemic (Ma and Earn, 2006).

In order to understand the effect of testing processes on an epidemic dynamics, we deveopled a mechanistic SIR-type model with epidemic and testing components. This model provides a sensible platform to link the modeling of epidemic and testing components and study their interaction. Here, we studied the the effect of testing intensity, rate of test return and the isolation efficacy in reduction of the probability of transmission on the epidemic dynamics when different levels of testing "focus" (from random to highly targeted) are in place. Our model provides insights to the sensitivity of the epidemic dynamics, through $\mathcal{R}_0$, with respect to the undelying testing and isolation parameters.[**Ali:** *edited in response to David comments.*]

3 Methods

We developed a deterministic model, Eqs. (A1), which groups individuals based on disease status and testing status. Disease states include Susceptible, Infectious and Recovered (thus this is an SIR-type model), and testing status categorizes people as *untested*, waiting-for-*positive*, waiting-for-*negative*, or *confirmed positive* (Figure 1). Symbolically, the testing status of an individual in the disease compartment X, where $X \in \{S, I, R\}$, is reflected in the subscript, namely X_{u}, X_{p}, X_{n} and X_{c}, for *untested*, waiting-for-*positive*, waiting-for-*negative*, or *confirmed positive*, respectively. Note that the top-to-bottom order of the testing-based compartments of each disease-based compartmenet X in the flowchart (Figure 1) and the model equations (A1) should match. However, we switched X_{u} and X_{n} in the flowchart (Figure 1) for the sake of tidiness of the flowchart. Further, two 'accumulator' compartments, N and P, were also incorporated in the model in order to collect cumulative reported negative or positive tests. The model equations and details of calculation of the basic reproduction number $\mathcal{R}_0$ are presented in the appendix (see Sec. 5.1).

Table 1 defines the model parameters, which are generally straightforward *per capita* flows between compartments, or modifiers to these flow rates. The novel component of the model comes in through the compartment-specific relative testing weights w_S, w_I and w_R; these give the relative rates at which people in the S, I, and R compartments are tested, respectively. Thus, we can spesify different levels of testing "focus" from random to highly targeted. For example, $w_I/w_S = 2$ means that infected individuals are tested at twice the *per capita* rate of susceptible individuals.

In order to link to more applied models, we constructed this model so we could specify the total *per capita* testing rate. We do this by defining the weighted size of the testing pool $W = w_S S_{\mathrm{u}} + w_I I_{\mathrm{u}} + w_R R_{\mathrm{u}}$, and calculating a scaling parameter for testing as:

$$\sigma = \frac{\rho N_0}{W}, \tag{1}$$

where ρ is the *per capita* testing intensity for population and defined as the number of daily tests taken in a population of size N_0. Thus, the *per capita* testing rate for compartment X is

$$F_X = \sigma w_X, \text{ where } X \in \{S, I, R\}. \tag{2}$$

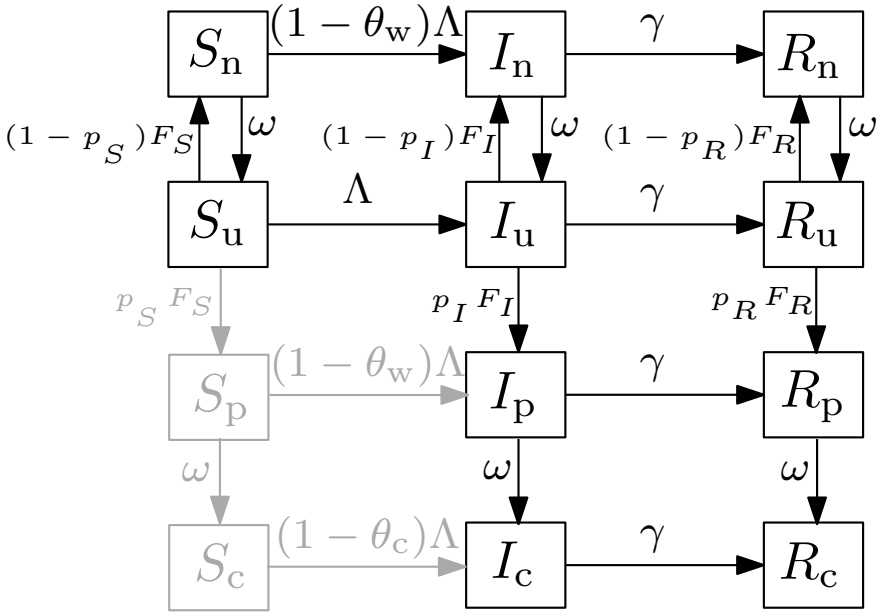

Figure 1: Flowchart of the SIR (Susceptible-Infectious-Recovered) model, A1. Here, the disease-based status of a compartment X, where $X \in \{S, I, R\}$, is combined with the testing-based status including X_{u}, X_{p}, X_{n} and X_{c}, for *untested*, waiting-for-*positive*, waiting-for-*negative*, or *confirmed positive*, respectively. Also, Λ is the force of infection with definition in Eq. (3), γ is the recovery rate, ω is the rate of test return, F_X (defined in Eq. (2)) and p_X represent the *per capita* testing rate and the probability of positive tests, respectively, for compartment X. For further description of the parameters see Table 1.

For a high-sensitivity test, infected people typically flow through to the "confirmed positive" (I_c, R_c) compartments and are thus unavailable for further testing. Over the course of the epidemic, a fixed testing rate as specified in (1) can (if large enough) exhaust the pool of people available for testing, leading to a singularity when no one is left untested. Although this phenomenon does not affect our analysis of $\mathcal{R}_0$, it can affect the temporal dynamics (we discuss an adjustment to the model that solves this problem in the appendix).

The classical SIR model is based on the following implicit assumptions; well-mixed population, homogeneity of the population (i.e., all individuals are equaly susciptable and equaly infectious for the same length of time when infected), exponentially distributed duration of infection and large population size (see, e.g., Keeling and Rohani (2011)). In addition to these standard assumptions, our model, A1, assumes: (i) there is a single force of infection (new cases per unit time), Λ, defined as follows

$$\Lambda = \frac{\beta}{N_0}\big(I_u + (1-\theta_w)(I_n + I_p) + (1-\theta_c)I_c\big), \tag{3}$$

across all susceptible pools with transmission rate β and isolation efficacy in reduction of the probability of transmission for three testing-based compartments "waiting" and *confirmed positive* individuals, θ_w and θ_c respectively, (see Table 1 for further details), (ii) $\theta_w \leq \theta_c$, i.e., the individuals awaiting test results have a higher transmission probability than the reported individuals. Thus, for instance when the awaiting people follow the isolation perfectly, θ_w is closer to 1, while when they less follow the isolation, θ_w is closer to 0. For this analysis, we also assume a perfectly specific test ($p_S = 0$). This last assumption combined with the assumption that no susceptible individual is in waiting-for-*positive* or *confirmed positive* compartments, i.e., $S_p(0) = S_c(0) = 0$, reduces the model to 10 equations where equations c and d in model (A1) are eliminated.

The Disease-Free Equilibrium (DFE) for the SIR model, Eqs. (A1), is found by setting the infected compartments to 0 and solving for the unknowns. The DFE is

$$S_n^* = \frac{\rho}{\omega} N_0, \;\; S_u^* = \frac{\omega - \rho}{\omega} N_0, \;\text{ and } I_j = R_j = 0 \text{ for all } j. \tag{4}$$

The corresponding *per capita* testing rate (Eq. 2) for the infected compartment I at DFE is one of the key analysis parameters and can be simplified as

$$\hat{F}_I = (\omega\rho/(\omega - \rho))w_I/w_S. \tag{5}$$

The basic reproduction number, $\mathcal{R}_0$, was calculated by using the next generation matrix method developed by van den Driessche and Watmough (2002). $\mathcal{R}_0$ is

$$\mathcal{R}_0 = \frac{\beta}{\gamma}(1-\Delta), \tag{6}$$

where the term $\frac{\beta}{\gamma}$ is the classical basic reproduction number for a SIR model without testing and isolation (see, e.g., Keeling and Rohani (2011)), and Δ is the reduction parameter defined as follows. [**Ali:** *Δ should be updated, the expression will be linear in θ_c but quadratic in*

Symbol	Description	Unit	Value
N_0	Total population size	people	10^6
ω	Rate of test return, i.e., rate of onward flow from "waiting" to "confirmed" or "untested" compartments	1/day	-
γ	Recovery rate	1/day	1/3
ρ	*per capita* testing intensity	1/day	-
θ_{w}	Isolation efficacy in reduction of the probability of transmission for "waiting" individuals	-	-
θ_{c}	Isolation efficacy in reduction of the probability of transmission for "confirmed positive" individuals	-	-
β	Transmission rate	1/day	0.339
Λ	Force of infection	1/day	-
p_S	Probability of positive tests for S $(= 1 - \text{specificity})$	-	0
p_I	Probability of positive tests for I $(= \text{sensitivity})$	-	1
p_R	Probability of positive tests for R $(= 1 - \text{specificity})$	-	0.5
w_S, w_I, w_R	Relative testing weights	-	Random: $\{1, 1, 1\}$ Targeted: $\{0.3, 1, 1\}$

Table 1: Parameters of the model (A1).

θ_w, C stay unchanged. It can be proved that Δ increases in θ_w for feasible range of θ_w (I think this argument will go to the appendix).?]

$$\Delta = (A\ \theta_w + B\ \theta_c)/C, \tag{7}$$

where

$$\begin{aligned} A =& \gamma\Big(\big(\gamma(\omega+\gamma)+\omega p_I\hat{F}_I\big)\frac{(1-\theta_w)S_n^*}{N_0}+(\omega+\gamma)\hat{F}_I\Big),\\ B =& \omega p_I(\gamma\frac{S_u^*}{N_0}+\omega)\hat{F}_I,\\ C =& (\omega+\gamma)\Big(\gamma(\omega+\gamma)+(\gamma+\omega p_I)\hat{F}_I\Big). \end{aligned} \tag{8}$$

Further details of derivation of $\mathcal{R}_0$ are provided in section 5.1 of the appendix. Note that Δ has been presented in a specific monotonic form with respect to isolation efficacy parameters, θ_w and θ_c, in order to simplify showing one of the results of this paper which is the reduction effect of isolation on $\mathcal{R}_0$. Further, we represent Δ in another equivalent form in the appendix (Sec. 5.2) to show the nontrivial-nonmonotonic effect of testing intensity and test return rate on $\mathcal{R}_0$.

The analytical calculation of the next-generation matrix and simplifying the expression of $\mathcal{R}_0$ was carried out in Maple (Maplesoft, 2010). We used R (R Core Team, 2020) for simulations, in particular, for plotting the contours of Δ (7) over a range of selected set of parameters of interest, i.e., parameters that could be manipulated by public-health policy. These parameters include the isolation efficacy parameters, θ_c and θ_w, *per capita* testing intensity, ρ, and the rate of test return, ω. The rest of model parameters kept fixed at sensible values (see Table 1 for the parameter values). Note that all plots are illustrated in the scale of the mean test return time $1/\omega$ (day). Results are shown in Fig. 2 and Fig. 3 with two panels; panel (a) represents the random testing, thus $w_S = w_I = w_R = 1$, and panel (b) represents targeted testing, thus $w_S = 0.3$ and $w_I = w_R = 1$. To illustrate the changes in $\mathcal{R}_0$ with respect to *per capita* testing intensityρ, two sets of plots are presented. Fig. 2 reflects the changes in $\mathcal{R}_0$ when ρ is small relative to the population size. Specifically, $\rho \in [0, 0.01]$, and the test return rate $\omega \in [0.1, 2]$. This is a more realistic scenario of testing as we have observed in COVID-19 pandemic. That is, 1% of a population are tested per day at maximum capacity, so in a population of size $N_0 = 10^6$, 10000 individuals will be tased per day at maximum. In order to illustrate the non-monotonic changes in $\mathcal{R}_0$ with respect to ρ, Fig. 3 with maximum capacity of ρ is larger relative to the population size, $\rho \in [0, 0.5]$, and the test return rate $\omega \in (0.5, 2]$. In both Fig. 2 and Fig. 3, the isolation efficacy parameters, θ_w and θ_c vary from 0 to 1. Note that the critical contour of $\Delta = 1 - \frac{\gamma}{\beta}$, corresponding to the threshold $\mathcal{R}_0 = 1$, is plotted in solid line in the panels. Thus, a combination of ρ and ω above this critical contour results in reducing $\mathcal{R}_0$. Also realize that $\mathcal{R}_0 = \frac{\beta}{\gamma}$, about 1.017 here, for the classical SIR model which can be acheived in the context of our model when $\rho = 0$, no testing, or $\theta_w = \theta_w = 0$, no isolation.

4 Results

The explicit formula for the basic reproduction number, $\mathcal{R}_0$ (6), provides an opportunity to study the influence of changes in the underlying parameters of interest on the critical index

of epidemic dynamics. These parameters include the isolation efficacy parameters, θ_c and θ_w, *per capita* testing intensity, ρ, and the rate of test return, ω. In this context, two testing strategies, namely random and targeted testing, were explored.

Examining our formula for $\mathcal{R}_0$ (6) gives the following results. See the appendix, Sec. 5.2 and Sec. 5.3 for details.

1. Increasing the isolation parameters for tested and confirmed individuals decreases $\mathcal{R}_0$;
2. Higher testing ρ intensity always decreases $\mathcal{R}_0$ **if**: testing is random; **or** ρ is small.
3. A higher rate of test return always decreases $\mathcal{R}_0$, **if** $\theta_w = 0$.

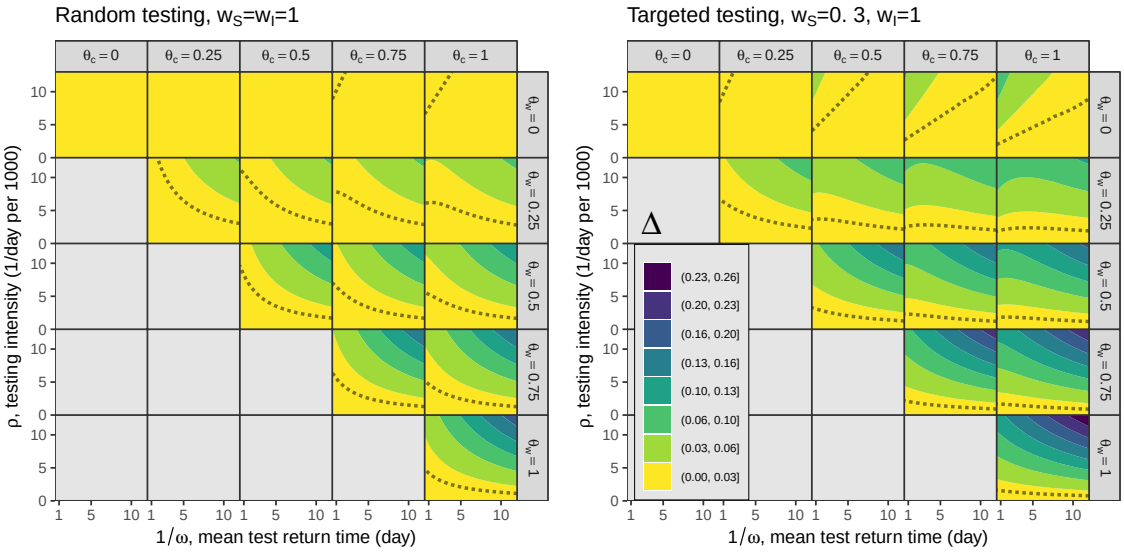

(a) (b)

Figure 2: **A comparison of the behaviour of the basic reproduction number, $\mathcal{R}_0$, between random versus targeted testing strategies at different levels of testing and isolation.** We numerically evaluate Δ (6), reflecting the reduction of $\mathcal{R}_0$ with respect to testing and isolation. We use the following parameters (see Table 1): $N_0 = 1 \times 10^6$, $\omega \in [0.1, 2]$ 1/day, $1/\gamma = 3$ days, $\rho \in [0, 0.01]$ 1/day, θ_w and θ_c vary between 0 and 1 with 0 for no effect and 1 for full effect of isolation on the transmission probability, $\beta = 0.339$ 1/day, $p_S = 0$, $p_I = 1$ and $p_R = 0.5$. Contours of Δ are plotted for two testing strategies identified by a set of relative testing weights; (a) random testing where $w_S = w_I = w_R = 1$ and (b) targeted testing where $w_S = 0.3$ and $w_I = w_R = 1$. The black dotted line in each panel represents the critical contour of $\Delta = 1 - \frac{\gamma}{\beta}$, i.e., the Δ corresponding to the threshold of $\mathcal{R}_0 = 1$.

Numerical results are shown in Fig. 2. Targeted testing (panel b) is more effective at control than random testing (panel a).

When $\theta_w = 0$ (top row of each panel), we see that shorter test-waiting times reduce $\mathcal{R}_0$ (Δ increases as we move to the left in each plot in this row). For non-zero Δ, however,

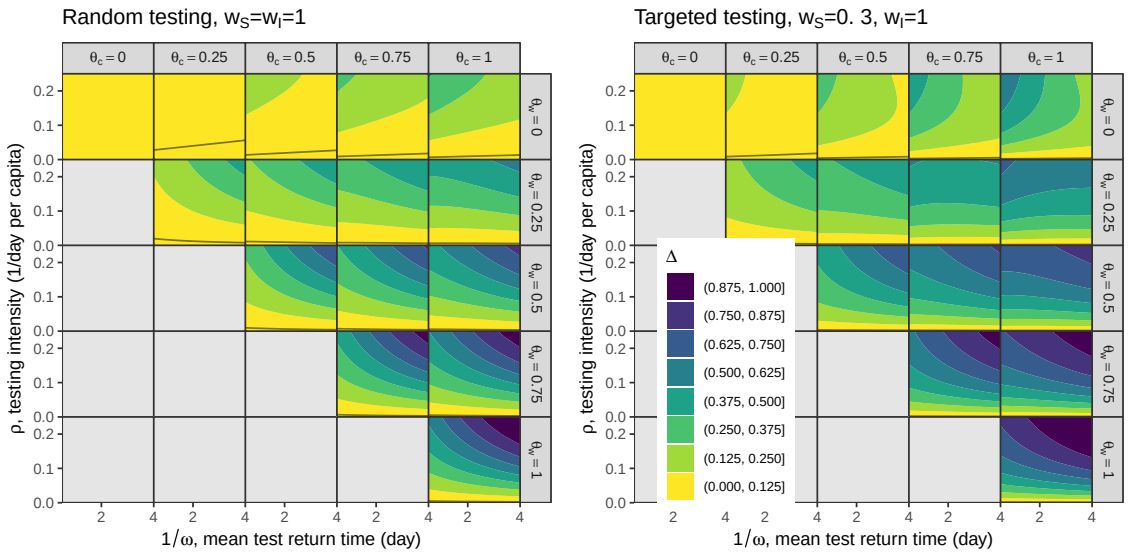

(a) (b)

Figure 3: **A comparison of the behaviour of the basic reproduction number, $\mathcal{R}_0$, between random versus targeted testing strategies at different levels of testing and isolation.** We numerically evaluate Δ (6), reflecting the reduction of $\mathcal{R}_0$ with respect to testing and isolation. We use the following parameters (listed in Table 1): $N_0 = 1 \times 10^6$, $\omega \in (0.25, 2]$ 1/day, $1/\gamma = 3$ days, $\rho \in [0, 0.25]$ 1/day, $\theta_{\rm w}$ and $\theta_{\rm c}$ vary between 0 and 1 with 0 for no effect and 1 for full effect of isolation on the transmission probability, $\beta = 0.339$ 1/day, $p_S = 0$, $p_I = 1$ and $p_R = 0.5$. Contours of Δ are plotted for two testing strategies identified by a set of relative testing weights; (a) random testing where $w_S = w_I = w_R = 1$ and (b) targeted testing where $w_S = 0.3$ and $w_I = w_R = 1$. The black solid line in each panel represents the critical contour of $\Delta = 1 - \frac{\gamma}{\beta}$, i.e., the Δ corresponding to the threshold of $\mathcal{R}_0 = 1$. [**BMB:** *we still have some collisions in the y-axis tick labels*]

we mostly see the opposite effect: less waiting leads to more transmission. This is because returning negative tests leads people to stop distancing; this applies both to susceptibles, and to infectious people who receive negative test results because they were sampled when susceptible (or because of imperfect test sensitivity, which is not modeled in this figure).

We also see that greater test intensity ρ increases the effectiveness of control Δ (Δ increases as we move up in each plot in this Figure. Mathematically speaking, we did find a counter-vailing effect, but this can only be seen when we allow ρ to take unrealistically large values, and only for weighted testing (see Fig. 3). The explanation here is that more rapid testing leaves more susceptibles in the "waiting-for-no" category at the DFE; these people must then wait for their tests to be returned before they can be tested again, receive a positive test, and become cautious. This effect is usually weak compared to the helpful effects of testing, but if testing is weighted, θ_w is low, and test returns are slow, t is possible for increasing ρ to reduce Δ (see upper-right part of upper-right plot of Fig. 3(b)).

5 Discussion

Mathematical modeling of infectious disease outbreaks provides insights on how testing processes influence the epidemiological processes through isolation. Here, we develop a compartmental SIR-type model to study the potential effect of testing strategies, testing intensity, test sensitivity and specificity, test reporting time and isolation on epidemic dynamics. While targeted testing strategies, including targeting people with infection-like symptoms or the contacts of confirmed cases, are always more effective than random testing, as expected, we find that in some cases the direct effect of testing is that viral spread is greater for a slow test than for a fast test. This counter-intuitive effect can occur when people are cautious when awaiting a test result, and may not be robust to second-order effects of fast testing (such as better contact tracing). [**Ali:** *this is a valid sentence especially when θ_w is closer to 1, but not sure if this was counter-intuitive or was the opposite of it? i.e., that viral spread is greater for a fast test ($1/\omega$ closer to 0) than for a slow test.*]

We incorporated the compartment-specific relative testing weights, w_S, w_I and w_R, to model random testing and *targeted* testing strategies. Here, in the case of targeted testing and for the simplicity and illustration purposes, we assumed that infected and recovered individuals are tested at three times the *per capita* rate of susceptible individuals, thus $w_I/w_S = 3$ and $w_R = w_I$. Note that we have not specified a methodology to assign particular relative testing weights corresponding to a particular targeted testing scenario. Modeling different targeted testing strategies, equivalently test-specific testing weights in our framework, requires prior information of the conditional probabilities of getting tested for people in a given compartment. This can be implied when we would like to quantify and compare the effect of different levels of test focus for infectious people on the basic reproduction number $\mathcal{R}_0$, and conclude about the disease spread management. For example, when people are tested for "screening", the individuals with potential higher mobility, eg. people who are getting on flights, get more tested and thus the coresponding heavier testing weight is assigned than people awaiting for a surgery and are probably going to stay in a long-term-care facility and consequently less mobile and more isolated to begin with. With our model, we would be able to compare the sensitivity of the disease dynamics, through $\mathcal{R}_0$, with respect to testing different high-risk groups in the population. This part needs to be developed further in future work.

The *per capita* testing intensity, ρ; Proposition 2 and also Figures 2 and 3 indicates that increasing testing intensity ρ may reduce $\mathcal{R}_0$ but there is a counter-intuitive machanism. The expected mechanism was that as more untested infected individuals are moved to the test compartments, i.e., from I_u to I_p and I_n, and eventually to the confirmed compartment I_c, they may partially or fully self-isolate (θ_w and θ_c varies between 0 and 1 with $\theta_w \leq \theta_c$). Thus, the higher the *per capita* testing intensity ρ, the lower the force of infection (3) and the lower $\mathcal{R}_0$ will become. This is true when ρ is very small relative to N_0 and can be verified analytically and through our simulation. The counter-intuitive mechanism is that at the DFE, higher *per capita* testing intensity, may delay recognition of true infected individuals I_p and causing an increase in $\mathcal{R}_0$ as follows. At high ρ, more people will be moved from S_u^* to S_n^*, thus a higher proportion of awaiting people may get infected and end up in I_n, and be delayed from being eligable for retesting I_u and eventually to I_p and I_c. Our analysis (Sec. 5.2) and simulation (see Fig. 3 panel (b) when $\theta_c = 1$ and $\theta_w = 0$) support such a

mechanism. In particular, if (**??**) holds we will have such a result.

The potential advantage of slow test reporting, or favorable-delay-reporting; Individuals are highly likely to fully self-isolate when they are either awaiting the test results or they are reported, thus reducing or eliminating their potentially infectious contacts. Thus, the faster the test reporting rate, ω, the shorter these individuals stay in the "*safe*" awaiting-confirmed compartments, namely X_n, X_p and X_c for $X \in \{S, I, R\}$, and the more they get involved in the infection process. This advantage of slow test reporting is real, and neglected. We also compare to an individual-level advantage of fast tests: people who test positive may be even more careful. In our model analysis, Proposition **??** part 3 is describing this potential advantage. It states that returning test results more rapidly, i.e., increasing the rate ω, does not necessarily lower the reproduction number $\mathcal{R}_0$; whether increasing ω lowers $\mathcal{R}_0$ depends on the precise combination of model parameters including test reporting rate, testing strategies represented by compartment-specific testing weights, test sensitivity and specificity, and the level of isolation. Specifically, in the case of perfect isolation, i.e., when $\theta_w = 1$ and $\theta_c = 1$, $\mathcal{R}_0$ may increase as the test reporting process becomes faster. This can be seen from expression (**??**). Another example of this favorable delay in ω could be when the test being employed produces many false negatives. Because many infected asymptomatic individuals will believe they are uninfected/uninfectious, thus may unknowingly spread the virus to many others. Again the delay in the test reporting rate keeps these individuals in the "*safe*" awaiting-confirmed compartments.

we are missing out on community-level advantages of fast testing: better assessment of the situation, identification of hot spots, contact-tracing, etc. The *per capita* testing intensity of CIVID-19 after about a year from the first case reported in December 2019, is still low ($(\rho \approx 0)$ in our model). In near future new test kits may be widely accessible, our model provide insights in this case. In particular, if a cheap test can identify on average more infected individuals as an expensive test, then our model predicts that the cheap test will lower $\mathcal{R}_0$ more. In contrast, if an expensive test can identify on average more infected individuals, it will not necessarily lower $\mathcal{R}_0$ more than the cheap test. The use of tests cheaper than RT-PCR has been proposed as a potential strategy for containing the COVID pandemic. While cheaper tests may be less sensitive and reliable than RT-PCR, they allow for broader and more intense testing. Using our Taylor approximation of $\mathcal{R}_0$ near $\rho = 0$, we examined what circumstances (i.e., model parameters) make the use of one test more favourable than another, and give a complete description through inequality A38. In general, we found that the expensive test tends to more effectively lower $\mathcal{R}_0$ when (a) individuals who test positive self-isolate much more than individuals who are waiting for their test result, (b) the time it takes to return tests is much shorter than the mean infectious period, and (c) the testing intensity is much greater for infected individuals than susceptible individuals.

[**Ali:** *not sure if we want these 2 following parageraphs, or shrink it into afew short sentences?*] In addition to the favorable-delay-reporting observation of our model (A1), the model enables us to quantify the amount of delay required in the test reporting process as a strategy to reduce $\mathcal{R}_0$. To give a biological interpretation, we describe the qualitative trends predicted by the inequality (A37). To summarise, returning test results more rapidly tends to be favourable (i.e., reduces $\mathcal{R}_0$) when (i) *Confirmed-positive* individuals, lower their contact much more than individuals who are waiting for their test results (i.e., $\theta_c \gg \theta_w$), (ii) the test is highly sensitive (i.e., p_I is close to 1), and (iii) the targeted testing strategy is

used (i.e., $w_I \gg w_S$).

one point we can make when discussing the relative weight of testing in different compartments is to discuss pre-testing screening tools, such as surveys or questionnaires. If we have a quantitative description of how the testing intensities affect the dynamics, we can make statements like "our results suggest that employing a pre-testing screening tool can help target infected individuals more effectively. In particular, doubling the sensitivity of the pre-screening tool would *do something* to $\mathcal{R}_0$.

[**DJDE:** *Some of this reads like notes for discussion rather than text for the paper, so I'm not trying to edit.*]

References

Dietz, K. (1993). The estimation of the basic reproduction number for infectious diseases. *Statistical methods in medical research*, 2(1):23–41.

Foddai, A., Lubroth, J., and Ellis-Iversen, J. (2020). Base protocol for real time active random surveillance of coronavirus disease (COVID-19)–adapting veterinary methodology to public health. *One Health*, page 100129.

Graubard, B. I. and Korn, E. L. (1996). Modelling the sampling design in the analysis of health surveys. *Statistical methods in medical research*, 5(3):263–281.

Keeling, M. J. and Rohani, P. (2011). *Modeling infectious diseases in humans and animals*. Princeton University Press.

Ma, J. and Earn, D. J. D. (2006). Generality of the final size formula for an epidemic of a newly invading infectious disease. *Bulletin of Mathematical Biology*, 68(3):679–702.

Maplesoft (2010). *Maple (14)*. a division of Waterloo Maple Inc., Waterloo, Ontario.

R Core Team (2020). *R: A Language and Environment for Statistical Computing*. R Foundation for Statistical Computing, Vienna, Austria.

Shaw, C. L. and Kennedy, D. A. (2021). What the reproductive number R0 can and cannot tell us about COVID-19 dynamics. *Theoretical Population Biology*.

van den Driessche, P. and Watmough, J. (2002). Reproduction numbers and sub-threshold endemic equilibria for compartmental models of disease transmission. *Mathematical biosciences*, 180(1-2):29–48.

Appendix

5.1 Model and calculation of $\mathcal{R}_0$

The model in the form of a system of ordinary differential equations is

$$
\begin{aligned}
dS_{\mathrm{u}}/dt &= -\Lambda S_{\mathrm{u}} - F_S S_{\mathrm{u}} + \omega S_{\mathrm{n}}, && \text{(A1a)}\\
dS_{\mathrm{n}}/dt &= -(1-\theta_{\mathrm{w}})\Lambda S_{\mathrm{n}} + (1-p_S)F_S S_{\mathrm{u}} - \omega S_{\mathrm{n}}, && \text{(A1b)}\\
dS_{\mathrm{p}}/dt &= -(1-\theta_{\mathrm{w}})\Lambda S_{\mathrm{p}} + p_S F_S S_{\mathrm{u}} - \omega S_{\mathrm{p}}, && \text{(A1c)}\\
dS_{\mathrm{c}}/dt &= -(1-\theta_{\mathrm{c}})\Lambda S_{\mathrm{c}} + \omega S_{\mathrm{p}}, && \text{(A1d)}\\
dI_{\mathrm{u}}/dt &= \Lambda S_{\mathrm{u}} - F_I I_{\mathrm{u}} + \omega I_{\mathrm{n}} - \gamma I_{\mathrm{u}}, && \text{(A1e)}\\
dI_{\mathrm{n}}/dt &= (1-\theta_{\mathrm{w}})\Lambda S_{\mathrm{n}} + (1-p_I)F_I I_{\mathrm{u}} - \omega I_{\mathrm{n}} - \gamma I_{\mathrm{n}}, && \text{(A1f)}\\
dI_{\mathrm{p}}/dt &= (1-\theta_{\mathrm{w}})\Lambda S_{\mathrm{p}} + p_I F_I I_{\mathrm{u}} - \omega I_{\mathrm{p}} - \gamma I_{\mathrm{p}}, && \text{(A1g)}\\
dI_{\mathrm{c}}/dt &= (1-\theta_{\mathrm{c}})\Lambda S_{\mathrm{c}} + \omega I_{\mathrm{p}} - \gamma I_{\mathrm{c}}, && \text{(A1h)}\\
dR_{\mathrm{u}}/dt &= \gamma I_{\mathrm{u}} - F_R R_{\mathrm{u}} + \omega R_{\mathrm{n}}, && \text{(A1i)}\\
dR_{\mathrm{n}}/dt &= \gamma I_{\mathrm{n}} + (1-p_R)F_R R_{\mathrm{u}} - \omega R_{\mathrm{n}}, && \text{(A1j)}\\
dR_{\mathrm{p}}/dt &= \gamma I_{\mathrm{p}} + p_R F_R R_{\mathrm{u}} - \omega R_{\mathrm{p}}, && \text{(A1k)}\\
dR_{\mathrm{c}}/dt &= \gamma I_{\mathrm{c}} + \omega R_{\mathrm{p}}, && \text{(A1l)}\\
dN/dt &= \omega(S_{\mathrm{n}} + I_{\mathrm{n}} + R_{\mathrm{n}}), && \text{(A1m)}\\
dP/dt &= \omega(I_{\mathrm{p}} + R_{\mathrm{p}}), && \text{(A1n)}
\end{aligned}
$$

where parameters are specified in Table 1. The next generation matrix for this model is $G = FV^{-1}$, where matrix F represents the inflow of new infection to the infected compartments and matrix V represents the flow in the infected compartments when the population is totally susceptible. Matrices F and V are

$$
\begin{aligned}
F =& \beta/N_0 \begin{bmatrix} S_{\mathrm{u}}^* & (1-\theta_{\mathrm{w}})\,S_{\mathrm{u}}^* & (1-\theta_{\mathrm{w}})\,S_{\mathrm{u}}^* & (1-\theta_{\mathrm{c}})\,S_{\mathrm{u}}^* \\ (1-\theta_{\mathrm{w}})S_{\mathrm{n}}^* & (1-\theta_{\mathrm{w}})^2\,S_{\mathrm{n}}^* & (1-\theta_{\mathrm{w}})^2\,S_{\mathrm{n}}^* & (1-\theta_{\mathrm{w}})(1-\theta_{\mathrm{c}})\,S_{\mathrm{n}}^* \\ 0 & 0 & 0 & 0 \\ 0 & 0 & 0 & 0 \end{bmatrix} && \text{(A2)}\\
=& \beta/N_0 \begin{bmatrix} S_{\mathrm{u}}^* \\ (1-\theta_{\mathrm{w}})S_{\mathrm{n}}^* \\ 0 \\ 0 \end{bmatrix} \begin{bmatrix} 1,\, 1-\theta_{\mathrm{w}},\, 1-\theta_{\mathrm{w}},\, 1-\theta_{\mathrm{c}} \end{bmatrix}, \text{and} && \text{(A3)}
\end{aligned}
$$

$$
V = \begin{bmatrix} \hat{F}_I + \gamma & -\omega & 0 & 0 \\ -(1-p_I)\hat{F}_I & \omega+\gamma & 0 & 0 \\ -p_I\hat{F}_I & 0 & \omega+\gamma & 0 \\ 0 & 0 & -\omega & \gamma \end{bmatrix}. \qquad \text{(A4)}
$$

The matrix inverse of V is

$$V^{-1} = \frac{1}{\gamma C}\begin{bmatrix} \gamma(\omega+\gamma)^2 & \gamma\omega(\omega+\gamma) & 0 & 0 \\ \gamma(\omega+\gamma)(1-p_I)\hat{F}_I & \gamma(\omega+\gamma)(\hat{F}_I+\gamma) & 0 & 0 \\ \gamma(\omega+\gamma)p_I\hat{F}_I & \gamma\omega p_I\hat{F}_I & C\gamma/(\omega+\gamma) & 0 \\ \omega(\omega+\gamma)p_I\hat{F}_I & \omega^2 p_I\hat{F}_I & C\omega/(\omega+\gamma) & C \end{bmatrix}, \tag{A5}$$

where $C = \big(\gamma(\omega+\gamma) + (\gamma+\omega p_I)\hat{F}_I\big)(\omega+\gamma)$ and $\hat{F}_I$ is the *per capita* testing rate for the infected people and represented in Eq. (5). Note that all the columns of matrix V^{-1} summ up to $1/\gamma$.

The particular form of F with two rows of zeros at the bottom results in the following blocked form of matrix G.

$$G = \begin{bmatrix} G_{11} & G_{12} \\ 0 & 0 \end{bmatrix}, \tag{A6}$$

where both blocked matricies G_{11} and G_{12} are 2 by 2. Given the upper triangular form of matrix G, the basic reproduction number $\mathcal{R}_0$ (defined as the spectral radius of matrix G) is only determined by the blocked matrix G_{11},

$$G_{11} = \frac{\beta}{\gamma\, C}\begin{bmatrix} (\omega-\rho)/\omega \\ (1-\theta_{\rm w})\rho/\omega \end{bmatrix}\begin{bmatrix} 1,\, 1-\theta_{\rm w},\, 1-\theta_{\rm w},\, 1-\theta_{\rm c} \end{bmatrix}\begin{bmatrix} \gamma(\omega+\gamma)^2 & \gamma\omega(\omega+\gamma) \\ \gamma(\omega+\gamma)(1-p_I)\hat{F}_I & \gamma(\omega+\gamma)(\hat{F}_I+\gamma) \\ \gamma(\omega+\gamma)p_I\hat{F}_I & \gamma\omega p_I\hat{F}_I \\ \omega(\omega+\gamma)p_I\hat{F}_I & \omega^2 p_I\hat{F}_I \end{bmatrix}. \tag{A7}$$

It is notable that matrix F (A2) has rank one and consequently G_{11} does so. That is G_{11} has only one non-zero eigenvalue which is $\mathcal{R}_0$.

The expression of $\mathcal{R}_0$ has a complicated form with all of the model parameters involved. This expression can be simplifed and represented given the specific form of matrix G_{11} (A7). For the purpose of simplicity we present $\mathcal{R}_0$ in the manuscript in terms of expressions A, B and C, specified in (8). This is intended to show that $\mathcal{R}_0$ decreases as the strength of isolation, shown by $\theta_{\rm w}$ and $\theta_{\rm c}$, increases.

It remains hard to show that the reproduction number $\mathcal{R}_0$ is decreasing with respect to *per capita* testing intensity, ρ, and the speed of the test return, ω, for the feasible ranges of the parameters, that is

$$\omega > 0, \tag{A8}$$

$$0 \le \rho < \omega, \tag{A9}$$

$$0 \le \theta_{\rm w} \le \theta_{\rm c} \le 1, \tag{A10}$$

$$\frac{w_I}{w_S} \ge 1. \tag{A11}$$

One way to do such an analysis is based on the fact that ρ is *per capita* rate so for a large population size, $N_0 \gg 1$, ρ is very small or close to 0, comparing to N_0. This provides a base to linearly approximate $\mathcal{R}_0$ when ρ is close to 0, and use this approximation to analyze

the behaviour of $\mathcal{R}_0$ with respect to ω (see section 5.3). In the next section we provide an equivalent representation of $\mathcal{R}_0$ to provide a ground to prove that more testing intensity decreases $\mathcal{R}_0$ for a general rane of parameters.

5.2 More testing intensity may decreases $\mathcal{R}_0$

This is to provide a mathematical materials to prove that $\frac{\partial}{\partial\rho}\Delta$ can be positive or negative, with Δ defined in Eq. (8), and thus $\frac{\partial}{\partial\rho}\mathcal{R}_0 < 0$, where $\mathcal{R}_0$ is the basic reproduction number, given in Eq. (6). We can rewrite matrix G_{11} in (A7) in the following form to simplify the calculations.

$$G_{11} = \frac{\beta}{\gamma\, C}\begin{bmatrix} S_{\rm u}^*/N_0 \\ (1-\theta_{\rm w})\, S_{\rm n}^*/N_0 \end{bmatrix}\begin{bmatrix} C - C_1, C - C_1 - C_2 \end{bmatrix}, \tag{A12}$$

where C is the same as the one in Eq. (8), i.e.,

$$C = (\omega+\gamma)(\gamma(\omega+\gamma) + (\omega\, p_I + \gamma)\,\hat{F}_I),$$

and C_1 and C_2 are

$$C_1 = (\omega+\gamma)(\theta_{\rm w}\,\gamma + \theta_{\rm c}\,\omega\, p_I)\hat{F}_I, \tag{A13}$$

$$C_2 = (\omega+\gamma)\gamma^2\,\theta_{\rm w} + (\theta_{\rm w} - \theta_{\rm c})\gamma\,\omega\, p_I\,\hat{F}_I, \tag{A14}$$

where $\hat{F}_I$ is given in Eq. (5). Note that for analysis brevity, we let $N_0 = 1$, thus $S_{\rm u}^*$ and $S_{\rm n}^*$ are in the scale of 0 to 1. $\mathcal{R}_0$ is in the same form as in Eq. (6)

$$\mathcal{R}_0 = \frac{\beta}{\gamma}(1-\Delta),$$

where

$$\Delta = \frac{1}{C}\big(C_1\, S_{\rm u}^* + ((C_1+C_2)(1-\theta_{\rm w}) + C\,\theta_{\rm w})\, S_{\rm n}^*\big). \tag{A15}$$

The first goal is to explore how changes in isolation, $\theta_{\rm w}$ and $\theta_{\rm c}$, affects $\mathcal{R}_0$. Mathematically we would like to verify the sign of $\frac{\partial\mathcal{R}_0}{\partial\theta_{\rm w}}$ and $\frac{\partial\mathcal{R}_0}{\partial\theta_{\rm c}}$. We start with simpliying Δ (A15) by factoring $\theta_{\rm w}$ and $\theta_{\rm c}$ in Eq. (A15). Thus, Δ can be rewritten as

$$\Delta = \frac{1}{C}\Big(- D_1\, S_{\rm n}^*\,\boldsymbol{\theta_{\rm w}^2} + \big(- \omega^2\, p_I\,\hat{F}_I\, S_{\rm n}^*\,\boldsymbol{\theta}_{\rm c} + D_2\, S_{\rm n}^* + \gamma\,\hat{F}_I(\omega+\gamma)\big)\boldsymbol{\theta}_{\rm w} + (\omega + \gamma\, S_{\rm u}^*)\omega\, p_I\,\hat{F}_I\,\boldsymbol{\theta}_{\rm c}\Big), \tag{A16}$$

where

$$D_1 = (\omega+\gamma)\gamma^2 + (\omega+\gamma+\omega\, p_I)\gamma\,\hat{F}_I, \tag{A17}$$

$$D_2 = (3\omega+2\gamma)\gamma^2 + (\omega+\gamma+2\omega\, p_I)\gamma\,\hat{F}_I + (\gamma + p_I\,\hat{F}_I)\omega^2. \tag{A18}$$

The scaled expression of Δ, specifically $\Delta\, C$, in Eq. (A16) is linear in $\theta_{\rm c}$ with a positive coefficient given by

$$(\gamma\, S_{\rm u}^* + \omega(1 - \theta_{\rm w}\, S_{\rm u}^*))\omega\, p_I\,\hat{F}_I.$$

This results in increasing Δ, thus decreasing $\mathcal{R}_0$ with respect to θ_c, that is $\frac{\partial \mathcal{R}_0}{\partial \theta_c} \leq 0$. Note that C is independant of θ_c and θ_w.

With a similar logic, the expression of $\Delta\, C$ derived from Eq. (A16) is a concave-down quadratic equation in θ_w, given by

$$-D_1\, S_n^*\, \boldsymbol{\theta_w^2} + \big(-\omega^2\, p_I\, \hat{F}_I\, S_n^*\, \boldsymbol{\theta}_c \,+\, D_2\, S_n^* \,+\, \gamma\, \hat{F}_I(\omega+\gamma)\big)\boldsymbol{\theta}_w. \tag{A19}$$

We show that the feasible range of θ_w lies btween 0 and the vertex of this parabola where the parabola is increasing in θ_w, and so does Δ which results in inferring $\frac{\partial \mathcal{R}_0}{\partial \theta_w} \leq 0$. It is enough to show that partial derivative of the expression (A19) with respect to θ_w at $\theta_w = 1$ is non-negative. It follows that

$$\frac{\partial \Delta}{\partial \theta_w}\, C\bigg|_{\theta_w=1} = (D_2 - 2D_1 - \omega^2\, p_I\, \hat{F}_I\, \theta_c)\, S_n^* + \gamma\, \hat{F}_I(\omega+\gamma) \tag{A20}$$

$$= (\gamma(\omega+\gamma) + \gamma\omega^2 + (1-\theta_c)\omega^2\, p_I\, \hat{F}_I)\, S_n^* + \gamma(\omega+\gamma)\, \hat{F}_I\, (1 - S_n^*), \tag{A21}$$

which is a positive quantity, given that θ_c and S_n^* vary between 0 and 1.

The second goal is to explore how changes in *per capita* testing intensity ρ affects $\mathcal{R}_0$. Mathematically we would like to verify the sign of $\frac{\partial \mathcal{R}_0}{\partial \rho}$, which specifically depends on $\frac{\partial \Delta}{\partial \rho}$. We use the derived expressions for S_u^* and S_n^*, given by Eqs. (4), in Δ (A16). Also, we define $\phi = \hat{F}_S = \frac{\rho\omega}{\omega - \rho}$, to reparametrize ρ. This is mainly to avoid singularity in $\hat{F}_I$ (5), when testing intensity ρ is very close to the rate of test return ω. Thus, ρ is reparametrized as

$$\rho = \frac{\omega\phi}{\omega + \phi}. \tag{A22}$$

This one-to-one monotonic reparametrization enables us to simplify the mathematical expressions and explore the simpler $\frac{\partial \Delta}{\partial \phi}$ instead of the complicated $\frac{\partial \Delta}{\partial \rho}$. The derivative is

$$\partial\Delta/\partial\phi = \frac{1}{d_3}(a_3\, \phi^2 + b_3\, \phi + c_3), \tag{A23}$$

where

$$a_3 = \frac{w_I}{w_S}\Bigg(\Big((\theta_w {p_I}^2 - \theta_c {p_I}^2 \theta_w)\omega^3 + (2\,\theta_w {p_I}^2 - \theta_c {p_I}^2 - p_I\, {\theta_w}^2 - \theta_c p_I\, \theta_w - {p_I}^2 {\theta_w}^2 + 2\,\theta_w p_I)\gamma\,\omega^2$$
$$+ (-2\, p_I\, {\theta_w}^2 - \theta_c p_I + 3\,\theta_w p_I - {\theta_w}^2 + \theta_w)\gamma^2\omega + (\theta_w - {\theta_w}^2)\gamma^3\Big)\frac{w_I}{w_S} + (-\theta_c p_I\, \theta_w + \theta_c p_I)\gamma\,\omega^2 +$$
$$(\theta_w + \theta_c p_I - {\theta_w}^2 - \theta_c p_I\, \theta_w)\gamma^2\omega + (\theta_w - {\theta_w}^2)\gamma^3\Bigg), \tag{A24}$$

$$b_3 = 2\frac{w_I}{w_S}(\omega+\gamma)\gamma\Big((\omega+\gamma+\omega\, p_I)(2-\theta_w)\,\gamma\,\theta_w + (1-\theta_w)\,\omega^2 p_I\theta_c + \omega^2 p_I\theta_w\Big), \tag{A25}$$

$$c_3 = (\omega+\gamma)^2\,\gamma\Big((2-\theta_w)\,\gamma^2\,\theta_w + (1+\frac{w_I}{w_S})\,\omega\,\gamma\,\theta_w + \frac{w_I}{w_S}\omega^2 p_I\theta_c\Big), \tag{A26}$$

$$d_3 = \frac{(\omega+\gamma)}{\omega}\Big((\omega p_I + \gamma)\frac{w_I}{w_S}\phi \,+\, (\omega+\gamma)\gamma\Big)^2(\omega+\phi)^2. \tag{A27}$$

Note that $\phi \geq 0$, also b_3, c_3 and d_3 are all positive. However a_3 can be positive or negative. If $a_3 \geq 0$, $\partial\Delta/\partial\phi \geq 0$ for all feasible range of parameters, thus $\frac{\partial}{\partial\rho}\mathcal{R}_0 \leq 0$. If $a_3 < 0$, then the quadratic expression in the numerator of (A23) has a positive root, ϕ^*, such that for $\phi > \phi^*$, $\partial\Delta/\partial\phi < 0$. An example of this counter-vailing effect of ρ on $\mathcal{R}_0$ occures when $\theta_{\rm w} = 0$ and $\theta_{\rm c} = 1$. This is illustraited in the top-right panel of the Fig. 3 panel (b), where the strength of isolation for awaiting people is the least, but the most for the confirmed cases. In this case

$$a_3 = \frac{w_I}{w_S}\,\omega\,\gamma\,p_I((\omega+\gamma) - \frac{w_I}{w_S}(\omega\,p_I + \gamma)).$$

Specifically, in the case of targeted testing which is identified with $\frac{w_I}{w_S} > 1$, and using a perfect sensative test, thus $p_I = 1$, there exists a range for ρ over which $\frac{\partial\mathcal{R}_0}{\partial\rho} \leq 0$. Note that ρ and ω have a similar mechanism in delaying people to get into $I_{\rm c}$, thus we would expect to see the non-trivial counter-vailing effect of these two parameters on $\mathcal{R}_0$.

5.3 rate of returning tests

The third goal is to explore how changes in the rate of test return ω affects $\mathcal{R}_0$. Mathematically we would like to verify the sign of $\frac{\partial\mathcal{R}_0}{\partial\omega}$, which specifically depends on $\frac{\partial\Delta}{\partial\omega}$. We use the linearization of $\mathcal{R}_0$ around $\rho = 0$ to show that there a non-monotonic relationship between $\mathcal{R}_0$ and ω. The taylor expansion of Δ at $\rho = 0$ is

$$\Delta = \frac{\rho}{\omega\,\gamma(\omega+\gamma)}\Big(\frac{w_I}{w_S}\,\omega^2\,p_I\,\theta_{\rm c} + (\frac{w_I}{w_S}+1)\,\gamma\omega\theta_{\rm w} + \gamma^2\,\theta_{\rm w}(2-\theta_{\rm w})\Big). \tag{A28}$$

This results in

$$\frac{\partial\Delta}{\partial\omega} = \frac{\rho}{\omega^2\,(\omega+\gamma)^2}\Big((p_I\,\frac{w_I}{w_S}\theta_{\rm c} - (1+\frac{w_I}{w_S})\theta_{\rm w})\omega^2 + 2\theta_w\,\gamma(\theta_w-2)\,\omega + \theta_w\,\gamma^2\,(\theta_w-2)\Big), \tag{A29}$$

around $\rho = 0$. [**Ali:** *I stoped here!*]

Perhaps counter-intuitively, the equation above does not predict that $\mathcal{R}_0$ is monotone decreasing with respect to ω. In other words; our model does not predict that returning test results more rapidly *always* lower $\mathcal{R}_0$. In order to gain insight into this intriguing behavior, we examine the zeroes of $\frac{\partial\mathcal{R}_0}{\partial\omega}(\omega)$. Defining the following quantity, Q, will help us write the roots of $\partial\mathcal{R}_0/\partial\omega$ neatly as follows.

$$Q = \frac{w_I}{w_S}\left(1 - \frac{n_t - 1}{n_w - 1}p_I\right). \tag{A30}$$

With that in mind, we can write the roots of $\partial\mathcal{R}_0/\partial\omega$ as

$$\omega_1 = \frac{\gamma}{-\sqrt{1-Q}-1} \tag{A31}$$

$$\omega_2 = \frac{\gamma}{\sqrt{1-Q}-1}. \tag{A32}$$

Note that the zeroes are real if and only if $Q < 1$. Note that have $\theta_{\rm c} > \theta_{\rm w}$, so if $p_I \approx 1$, we will have $Q < 0 < 1$. Thus, if we assume near-perfect test sensitivity, ω_1 and ω_2 will be real.

Assuming ω_1, ω_2 are real, it is easy to confirm that $\omega_1 < 0$ by looking at the denominator. To see that $\omega_2 > 0$, recall that $Q < 0$, so $\sqrt{1-Q} > 1$ and so $\sqrt{1-Q} - 1 > 0$. Knowing that $\omega_1 < 0$, the only root of interest (i.e., biologically relevant quantity) is ω_2.

We can prove that $\partial \mathcal{R}_0 / \partial \omega > 0$ when $\omega \in (0, \omega_2)$ and $\partial \mathcal{R}_0 / \partial \omega < 0$ when $\omega \in (\omega_2, \infty)$ by computing the limits of $\partial \mathcal{R}_0 / \partial \omega$ at 0 and ∞ respectively. So it follows that $\mathcal{R}_0$ has a global maximum with respect to ω at $\omega = \omega_2$.

Now we want to characterize the parameter regions on which $\partial \mathcal{R}_0 / \partial \omega < 0$ (i.e., the conditions under which returning test results more rapidly is favorable). By the previous analysis, this is equivalent to solving for $\omega > \omega_2$. So

$$\begin{aligned}
&\omega > \omega_2 \\
&\omega > \frac{\gamma}{\sqrt{1-Q} - 1} \\
&\sqrt{1-Q} > \frac{\gamma}{\omega} + 1 \qquad \text{(A33)} \\
&1 - Q > (\frac{\gamma}{\omega} + 1)^2. \qquad \text{(A34)}
\end{aligned}$$

Substituting in Q from (A30) we have

$$\begin{aligned}
&1 - \frac{w_I}{w_S}\left(1 - \frac{n_t - 1}{n_\omega - 1} P_i\right) > \left(\frac{\gamma}{\omega} + 1\right)^2 \qquad \text{(A35)} \\
&- \frac{w_I}{w_S}\left(1 - \frac{n_t - 1}{n_\omega - 1} P_i\right) > \left(\frac{\gamma}{\omega} + 1\right)^2 + 1 \qquad \text{(A36)} \\
&\frac{w_I}{w_S}\left(\frac{1 - n_t}{1 - n_\omega} P_i - 1\right) > \left(\frac{\gamma}{\omega} + 1\right)^2 + 1. \qquad \text{(A37)}
\end{aligned}$$

Since all steps in deriving (A37) are reversible, (A37) gives a necessary and sufficient condition for $\omega > \omega_2$, which characterizes when returning tests more rapidly would cause a decrease in $\mathcal{R}_0$.

5.4 On Testing Rate and Numerical Singularity

In this work, we didn't do any numerical solutions for the trajectories in our analysis. However, if one tries to do so there would be a singularity issue to deal with. Specifically, the numerical singularity issue with the chosen σ (1) is that the population in S compartments appeared to blow up when the DFE is achieved. This is once the only untested people are susceptibles, the FOI will become $\Lambda = 0$, testing rate $F_s = \rho N_0 / S_\mathrm{u}$. Thus, the first equation of the model (A1) will become $dS_\mathrm{u}/dt = -\rho N_0 + \omega S_\mathrm{n}$. Thus changes in S_u will be no longer dependent on S_u with a linear rate of leaving the S_u compartment. IN fact the testing rate, σ, should be formulated such that people from the untested compartments will not be tested if they are not there. One way to fix this issue, is to consider a maximum testing rate, τ (1/day). In general, we want to test at a rate of ρ across the whole population. This won't always be possible, so we impose a maximum rate of τ per testable person and redefine $\sigma = \frac{\tau \rho N_0}{\tau W + \rho N_0}$, with the assumption that $\tau \gg \rho$. This alteration in σ, does not change any results related to $\mathcal{R}_0$, thus we only impose it in the simulation of the epidemic dynamic.

5.5 Expensive vs. cheap tests

The use of tests cheaper than RT-PCR has been proposed as a potential strategy for containing the COVID-19 pandemic. While cheaper tests may be less sensitive and reliable than RT-PCR, they allow for broader and more intense testing. In the analysis below, we compare the $\mathcal{R}_0$ predicted by our model depending on the testing strategy.

Consider a test that allows us to test at rate ρ_1 and has sensitivity $P_{i,1}$, and another test that allows us to test at ρ_2 and has sensitivity $P_{i,2}$. Suppose that $\rho_1 > \rho_2$. Recall that the linearization of $\mathcal{R}_0$ around $\rho \approx 0$ is given by

$$\mathcal{R}_0 \approx \beta/\gamma + \frac{\beta\rho}{\omega(\omega+\gamma)\gamma^2 w_S}\Big(\gamma(-\theta_{\mathrm{w}})(\gamma w_S + \omega w_I) + (-\theta_{\mathrm{c}})p_I w_I \omega^2\Big).$$

Treating $\mathcal{R}_0$ as a function of ρ and P_i,we can reduce the inequality

$$\mathcal{R}_0(\rho_2, p_{I,2}) < \mathcal{R}_0(\rho_1, p_{I,1})$$

into

$$\begin{aligned}
&\rho_1\left(\gamma(-\theta_{\mathrm{w}})(\gamma w_S + \omega w_I) + (-\theta_{\mathrm{c}})p_{I,1} w_I \omega^2\right) - \rho_2\left(\gamma(-\theta_{\mathrm{w}})(\gamma w_S + \omega w_I) + (-\theta_{\mathrm{c}})p_{I,2} w_I \omega^2\right) > 0 \\
&\vdots \\
&\frac{\rho_2 P_{i,2} - \rho_1 P_{i,1}}{\rho_1 - \rho_2} > \frac{\theta_{\mathrm{w}}}{\theta_{\mathrm{c}}} \cdot \frac{\gamma(\gamma w_S + \omega w_I)}{\omega^2 w_I}
\end{aligned} \tag{A38}$$

Note that the RHS is positive, thus a necessary condition for the inequality above to hold is that $\rho_2 P_{i,2} > \rho_1 P_{i,1}$, equivalently

$$\frac{P_{i,2}}{P_{i,1}} > \frac{\rho_1}{\rho_2}. \tag{A39}$$

To state an example of this, if test A is three times as expensive as test B (and hence one can test three times as many people with test B), using test A rather than B will be favorable only if test A is at least 3 times more sensitive than test B. Note that this is a necessary but not sufficient condition, so even if test A is three times more sensitive, it is still possible for test B to be more effective.

Eq. (A38) tells us precisely when a test corresponding to $\rho_2, P_{i,2}$ will yield a lower $\mathcal{R}_0$ than a test corresponding to $\rho_1, P_{i,1}$, where $\rho_1 > \rho_2$. Some of the qualitative *trends* that favor test 2 (the higher-sensitivity test) include

- individuals who test positive self-isolate much more than individuals who are waiting for their test result.
- the time it takes to return tests is much shorter than the mean infectious period.
- the testing intensity is much greater for infected individuals than susceptible individuals.